Comparison of the Crystal and Electronic Structures of Three 2:1 Salts of the Organic Donor Molecule BEDT-TTF with Pentafluorothiomethylsulfonate Anions $SF_5CH_2SO_3^-$, $SF_5CHFSO_3^-$, and $SF_5CF_2SO_3^-$

Brian H. Ward, John A. Schlueter, Urs Geiser,* H. Hau Wang, Emilio Morales, James P. Parakka, Seddon Y. Thomas, and Jack M. Williams

Chemistry and Materials Science Divisions, Argonne National Laboratory, Argonne, Illinois 60439-4831

Paul G. Nixon, R. W. Winter, and Gary L. Gard

Department of Chemistry, Portland State University, Portland, Oregon 97207-0751

H.-J. Koo and M.-H. Whangbo

Department of Chemistry, North Carolina State University, Raleigh, North Carolina 27695-8204

Received April 26, 1999. Revised Manuscript Received November 23, 1999

Salts of the donor molecule, bis(ethylenedithio)tetrathiafulvalene (BEDT-TTF or ET), with pentafluorothiomethylsulfonate ($SF_5CX_2SO_3^-$, X = H or F) anions have been prepared. Three phases, β''-$(ET)_2SF_5CH_2SO_3$, β'-$(ET)_2SF_5CF_2SO_3$, and β''-$(ET)_2SF_5CHFSO_3$ were obtained by electrocrystallization with the corresponding $LiSF_5CX_2SO_3$ electrolytes. The structures of these salts were determined by single-crystal X-ray diffraction, and their physical properties were examined by electrical resistivity measurements as well as by ESR and Raman spectroscopy. The β''-$(ET)_2SF_5CH_2SO_3$, β''-$(ET)_2SF_5CHFSO_3$ and β'-$(ET)_2SF_5CF_2SO_3$ salts are considerably different in their crystal structures, physical properties, and electronic structures despite the similarity in the structures of the $SF_5CX_2SO_3^-$ (X = H, F) anions. The β''-$(ET)_2SF_5CH_2SO_3$ salt has two kinds of ET donor molecules with considerably different charge densities. The electronic structure of β''-$(ET)_2SF_5CHFSO_3$ has both one-dimensional (1D) and two-dimensional (2D) Fermi surfaces which are similar to those found in the organic superconductor β''-$(ET)_2SF_5CH_2CF_2SO_3$. The ESR data for the β'-$(ET)_2SF_5CF_2SO_3$ salt indicate that it opens a spin gap below 45 K. The differences in the physical properties of the three salts were analyzed by calculating the HOMO−HOMO interaction energies between nearest-neighbor ET molecules in their donor molecule layers.

I. Introduction

Since the discovery of superconductivity in $(TMTSF)_2ClO_4$,[1] where TMTSF refers to tetramethyltetraselenafulvalene, a large number of organic conductors and superconductors have been prepared. The organic donor molecule, bis(ethylenedithio)tetrathiafulvalene (BEDT-TTF or ET), has led to over 50 superconducting salts.[2,3] Among these salts, κ-$(ET)_2Cu[N(CN)_2]Br$ has the highest superconducting transition temperature T_c at ambient pressure (T_c = 11.6 K).[4] Superconducting ET salts with T_c approaching this record were obtained by using large perfluorinated anions $M(CF_3)_4^-$ (M = Cu, Ag, Au) (T_c = 2.1−11.1 K).[5−8] More recently, the first example of an organic superconductor containing both an organic cation and an organic anion, β''-$(ET)_2SF_5CH_2CF_2SO_3$, was discovered (T_c = 5.2 K).[9]

Many of the ET salts prepared with linear triatomic anions (I_3^-, IBr_2^-, AuI_2^-, I_2Br^-, $BrICl^-$, $IAuBr^-$, $AuBr_2^-$,

* To whom correspondence should be addressed.

(1) Bechgaard, K.; Carneiro, K.; Rasmussen, F. B.; Olsen, M.; Rindorf, G.; Jacobsen, C. S.; Pedersen, H. J.; Scott, J. C. *J. Am. Chem. Soc.* **1981**, *103*, 2440.

(2) Williams, J. M.; Ferraro, J. R.; Thorn, R. J.; Carlson, K. D.; Geiser, U.; Wang, H. H.; Kini, A. M.; Whangbo, M.-H. *Organic Superconductors (Including Fullerenes): Synthesis, Structure, Properties and Theory*; Prentice Hall: New Jersey, 1992.

(3) Ishiguro, T.; Yamaji, K. *Organic Superconductors*; Springer-Verlag: Berlin, Heidelberg, 1990.

(4) Kini, A. M.; Geiser, U.; Wang, H. H.; Carlson, K. D.; Williams, J. M.; Kwok, W. K.; Vandervoort, K. G.; Thompson, J. E.; Stupka, D. L.; Jung, D.; Whangbo, M.-H. *Inorg. Chem.* **1990**, *29*, 2555.

(5) Schlueter, J. A.; Carlson, K. D.; Geiser, U.; Wang, H. H.; Williams, J. M.; Kwok, W.-K.; Fendrich, J. A.; Welp, U.; Keane, P. M.; Dudek, J. D.; Komosa, A. S.; Naumann, D.; Roy, T.; Schirber, J. E.; Bayless, W. R.; Dodrill, B. *Physica (Amsterdam)* **1994**, *C233*, 379.

(6) Schlueter, J. A.; Williams, J. M.; Geiser, U.; Dudek, J. D.; Sirchio, S. A.; Kelly, M. E.; Gregar, J. S.; Kwok, W. K.; Fendrich, J. A.; Schirber, J. E.; Bayless, W. R.; Naumann, D.; Roy, T. *J. Chem. Soc., Chem. Commun.* **1995**, 1311.

(7) Schlueter, J. A.; Williams, J. M.; Geiser, U.; Dudek, J. D.; Kelly, M. E.; Sirchio, S. A.; Carlson, K. D.; Naumann, D.; Roy, T.; Campana, C. F. *Adv. Mater.* **1995**, *7*, 634.

(8) Schlueter, J. A.; Geiser, U.; Wang, H. H.; Kelly, M. E.; Dudek, J. D.; Williams, J. M.; Naumann, D.; Roy, T. *Mol. Cryst. Liq. Cryst.* **1996**, *284*, 195.

10.1021/cm990238q CCC: $19.00
Published on Web 01/25/2000

ICl_2^-, and $AuCl_2^-$)[2] exhibit a number of different crystal packing types (α, *β*, *κ*, *δ*, etc.). The *β*-type salts are further classified into three subgroups, i.e., *β*, *β*′, and *β*″.[2,10] The longer anions (e.g., I_3^-, IBr_2^-, AuI_2^-) tend to favor the *β*-type packing while the shorter anions favor the *β*′ and *β*″ motifs. The *β*-ET salts contain "face-to-face" stacks of ET donor molecules which form a 90° angle between the stacking axis and the ET molecular plane when projected along the long molecular axis. Also, *β*-$(ET)_2X$ (X = I_3^-, IBr_2^-, and AuI_2^-) salts[11−13] exhibit two-dimensional (2D) metallic behavior and become superconductors under ambient pressure.[10] The *β*′-ET cation−radical salts form with strongly dimerized, face-to-face ET molecules with the ET dimers along the stacking axis displaced from one another.[10] The *β*′-$(ET)_2X$ (X = ICl_2^-, $BrICl^-$, $AuCl_2^-$) salts have one-dimensional (1D) energy band structures and are magnetic semiconductors which undergo antiferromagnetic (AFM) phase transitions around 20−30 K.[14−16] In the *β*″-ET salts, the donor molecules within a stack are displaced slightly resulting in a ∼60° angle between the stacking axis and the ET molecular plane. The *β*″-type salts are typically 2D metals as found for *β*″-$(ET)_2X$ (X = $AuBr_2^-$, $IAuBr^-$, as well as several larger anions)[9,17−22] and several of them exhibit superconductivity, e.g., *β*″-$(ET)_2SF_5CH_2CF_2SO_3$ (T_c = 5.2 K),[9] *β*″-$(ET)_4(H_3O)Fe(C_2O_4)_3 \cdot C_6H_5CN$ (T_c = 7.0 K),[21] and *β*″-$(ET)_4(H_3O)Cr(C_2O_4)_3 \cdot C_6H_5CN$ (T_c = 6.0 K).[22]

In an attempt to prepare analogues of the superconductor, *β*″-$(ET)_2SF_5CH_2CF_2SO_3$, the carbon framework of the $SF_5CH_2CF_2SO_3^-$ anion[23,24] can be chemically modified both in the length of the carbon backbone and in the H and F atoms substitution pattern, to generate a number of similar anions, e.g., $SF_5CHFCF_2SO_3^-$, $SF_5CH_2SO_3^-$, $SF_5CF_2SO_3^-$, and $SF_5CHFSO_3^-$.[25] It is of interest to study how the structures and physical properties of the salts that these anions form with ET compare with those of the superconducting salt *β*″-$(ET)_2SF_5CH_2CF_2SO_3$. In the present work, we examine ET salts of three anions $SF_5CH_2SO_3^-$, $SF_5CF_2SO_3^-$, and $SF_5CHFSO_3^-$. These anions differ structurally only slightly by the CX_2 (X = H, F) substitution pattern. Nevertheless, the three new ET salts that we prepared, i.e., *β*″-$(ET)_2SF_5CH_2SO_3$, *β*″-$(ET)_2SF_5CHFSO_3$, and *β*′-$(ET)_2SF_5CF_2SO_3$, vary considerably in their crystal structures, physical properties, and electronic structures.

II. Experimental Section

Materials Synthesis. ET was synthesized[26] and the $LiSF_5CH_2SO_3$, $LiSF_5CF_2SO_3$, and $LiSF_5CHFSO_3$ salts were prepared by following the procedures reported in the literature.[25] Methylene chloride (99.6%, ACS HPLC grade) and 12-crown-4 ether were purchased from Aldrich Chemical Co. (Milwaukee, WI) and used without further purification. 1,1,2-Trichloroethane (TCE) was purchased from Acros (Chicago, IL) and distilled prior to use. The salts *β*″-$(ET)_2SF_5CH_2SO_3$, *β*′-$(ET)_2SF_5CF_2SO_3$, and *β*″-$(ET)_2SF_5CHFSO_3$ were grown by use of the electrocrystallization technique.[27,28] The electrochemical cells were assembled in an argon-filled drybox.

To prepare the $(ET)_2X$ (X = $SF_5CH_2SO_3$, $SF_5CF_2SO_3$, and SF_5CHFSO_3) salts, ET was loaded into the anode chamber of a two-electrode H-cell [0.018 mmol for *β*″-$(ET)_2SF_5CH_2SO_3$, 0.021 mmol for *β*′-$(ET)_2SF_5CF_2SO_3$, and 0.013 mmol for *β*″-$(ET)_2SF_5CHFSO_3$]. As solvent for ET and the salt LiX, methylene chloride was used for *β*″-$(ET)_2SF_5CH_2SO_3$ and *β*′-$(ET)_2SF_5CF_2SO_3$, and 1,1,2-trichloroethane for *β*″-$(ET)_2SF_5CHFSO_3$. A 15 mL solution saturated with LiX [0.21 mmol for *β*″-$(ET)_2SF_5CH_2SO_3$, 0.145 mmol for *β*′-$(ET)_2SF_5CF_2SO_3$, and 0.203 mmol for *β*″-$(ET)_2SF_5CHFSO_3$] and 10 drops of 12-crown-4 ether were added to both chambers of an H-cell. A current density of 0.19 $\mu A/cm^2$ was initially applied and gradually increased over a period of days to a higher value [i.e., 0.84 $\mu A/cm^2$ for *β*″-$(ET)_2SF_5CH_2SO_3$, 1.27 $\mu A/cm^2$ for *β*′-$(ET)_2SF_5CF_2SO_3$, and 0.29 $\mu A/cm^2$ for *β*″-$(ET)_2SF_5CHFSO_3$], at which time crystallization commenced. Crystals were grown at 25 °C on Pt wire electrodes for 19 days for *β*″-$(ET)_2SF_5CH_2SO_3$ and *β*′-$(ET)_2SF_5CF_2SO_3$, and 14 days for *β*″-$(ET)_2SF_5CHFSO_3$. Crystals of *β*″-$(ET)_2SF_5CH_2SO_3$ form as black, thin hexagonal plates, while crystals of *β*″-$(ET)_2SF_5CHFSO_3$ and *β*′-$(ET)_2SF_5CF_2SO_3$ form as long, black rods.

X-ray Structure Determination. Single-crystal X-ray diffraction data were collected at 298 K for *β*″-$(ET)_2SF_5CH_2SO_3$ and *β*″-$(ET)_2SF_5CHFSO_3$, and at 120 K for *β*′-$(ET)_2SF_5CF_2SO_3$ on a Siemens SMART single-crystal X-ray diffractometer equipped with a CCD-based area detector and a sealed tube X-ray source. Details are deposited as Supporting Materials.

Raman Spectroscopy. Raman spectra were recorded using a Raman microscope spectrometer (Renishaw, Ltd.) equipped with a He:Ne (λ_o = 6328 Å) laser. A low laser power of 0.06 mW focused on a 1 μm^2 area was applied. The spectra were averaged over 20 scans. Raman shifts between 50 and 2500 cm^{-1} were recorded and calibrated against the standard Si peak at 520 cm^{-1}.

(9) Geiser, U.; Schlueter, J. A.; Wang, H. H.; Kini, A. M.; Williams, J. M.; Sche, P. P.; Zakowicz, H. I.; Vanzile, M. L.; Dudek, J. D.; Nixon, P. G.; Winter, R. W.; Gard, G. L.; Ren, J.; Whangbo, M.-H. *J. Am. Chem. Soc.* **1996**, *118*, 9996.
(10) Mori, T. *Bull. Chem. Soc. Jpn.* **1998**, *71*, 2509.
(11) Yagubskii, É. B.; Shchegolev, I. F.; Laukhin, V. N.; Kononovich, P. A.; Kartsovnik, M. V.; Zvarykina, A. V.; Buravov, L. I. *Pis'ma Zh. Eksp. Teor. Fiz.* **1984**, *39*, 12.
(12) Williams, J. M.; Wang, H. H.; Beno, M. A.; Emge, T. J.; Sowa, L. M.; Copps, P. T.; Behroozi, F.; Hall, L. N.; Carlson, K. D.; Crabtree, G. W. *Inorg. Chem.* **1984**, *23*, 3839.
(13) Wang, H. H.; Beno, M. A.; Geiser, U.; Firestone, M. A.; Webb, K. S.; Nuñez, L.; Crabtree, G. W.; Carlson, K. D.; Williams, J. M.; Azevedo, L. J.; Kwak, J. F.; Schirber, J. E. *Inorg. Chem.* **1985**, *24*, 2465.
(14) Emge, T. J.; Wang, H. H.; Leung, P. C. W.; Rust, P. R.; Cook, J. D.; Jackson, P. L.; Carlson, K. D.; Williams, J. M.; Whangbo, M.-H.; Venturini, E. L.; Schirber, J. E.; Azevedo, L. J.; Ferraro, J. R. *J. Am. Chem. Soc.* **1986**, *108*, 695.
(15) Emge, T. J.; Wang, H. H.; Bowman, M. K.; Pipan, C. M.; Carlson, K. D.; Beno, M. A.; Hall, L. N.; Anderson, B. A.; Williams, J. M.; Whangbo, M.-H. *J. Am. Chem. Soc.* **1987**, *109*, 2016.
(16) Coulon, C.; Laversanne, R.; Amiell, J.; Delhaes, P. *J. Phys. C: Solid State Phys.* **1986**, *19*, L753.
(17) Ugawa, A.; Yakushi, K.; Kuroda, H.; Kawamoto, A.; Tanaka, J. *Chem. Lett.* **1986**, 1875.
(18) Mori, T.; Sakai, F.; Saito, G.; Inokuchi, H. *Chem. Lett.* **1986**, 1037.
(19) Kurmoo, M.; Talham, D. R.; Day, P.; Parker, I. D.; Friend, R. H.; Stringer, A. M.; Howard, J. A. K. *Solid State Commun.* **1987**, *61*, 459.
(20) Ugawa, A.; Okawa, Y.; Yakushi, K.; Kuroda, H.; Kawamoto, A.; Tanaka, J.; Tanaka, M.; Nogami, Y.; Kagoshima, S.; Murata, K.; Ishiguro, T. *Synth. Met.* **1988**, *27*, A407.
(21) Kurmoo, M.; Graham, A. W.; Day, P.; Coles, S. J.; Hursthouse, M. B.; Caulfield, J. L.; Singleton, J.; Pratt, F. L.; Hayes, W.; Ducasse, L.; Guionneau, P. *J. Am. Chem. Soc.* **1995**, *117*, 12209.
(22) Martin, L.; Turner, S. S.; Day, P.; Malik, K. M. A.; Coles, S. J.; Hursthouse, M. B. *Chem. Commun.* **1999**, 513.
(23) Canich, J. M.; Ludvig, M. M.; Gard, G. L.; Shreeve, J. M. *Inorg. Chem.* **1984**, *23*, 4403.
(24) Terejeson, R. J.; Mohtasham, J.; Gard, G. L. *Inorg. Chem.* **1988**, *27*, 2916.
(25) Hamel, N. N.; Nixon, P. G.; Gard, G. L.; Nafshun, R. L.; Lerner, M. M. *J. Fluorine Chem.* **1996**, *79*, 81.
(26) Mizuno, M.; Garito, A. F.; Cava, M. P. *J. Chem. Soc., Chem. Commun.* **1978**, 18.
(27) Emge, T. J.; Wang, H. H.; Beno, M. A.; Williams, J. M.; Whangbo, M.-H.; Evain, M. *J. Am. Chem. Soc.* **1986**, *108*, 8215.
(28) Stephens, D. A.; Rehan, A. E.; Compton, S. J.; Barkhau, R. A.; Williams, J. M. *Inorg. Synth.* **1986**, *24*, 135.

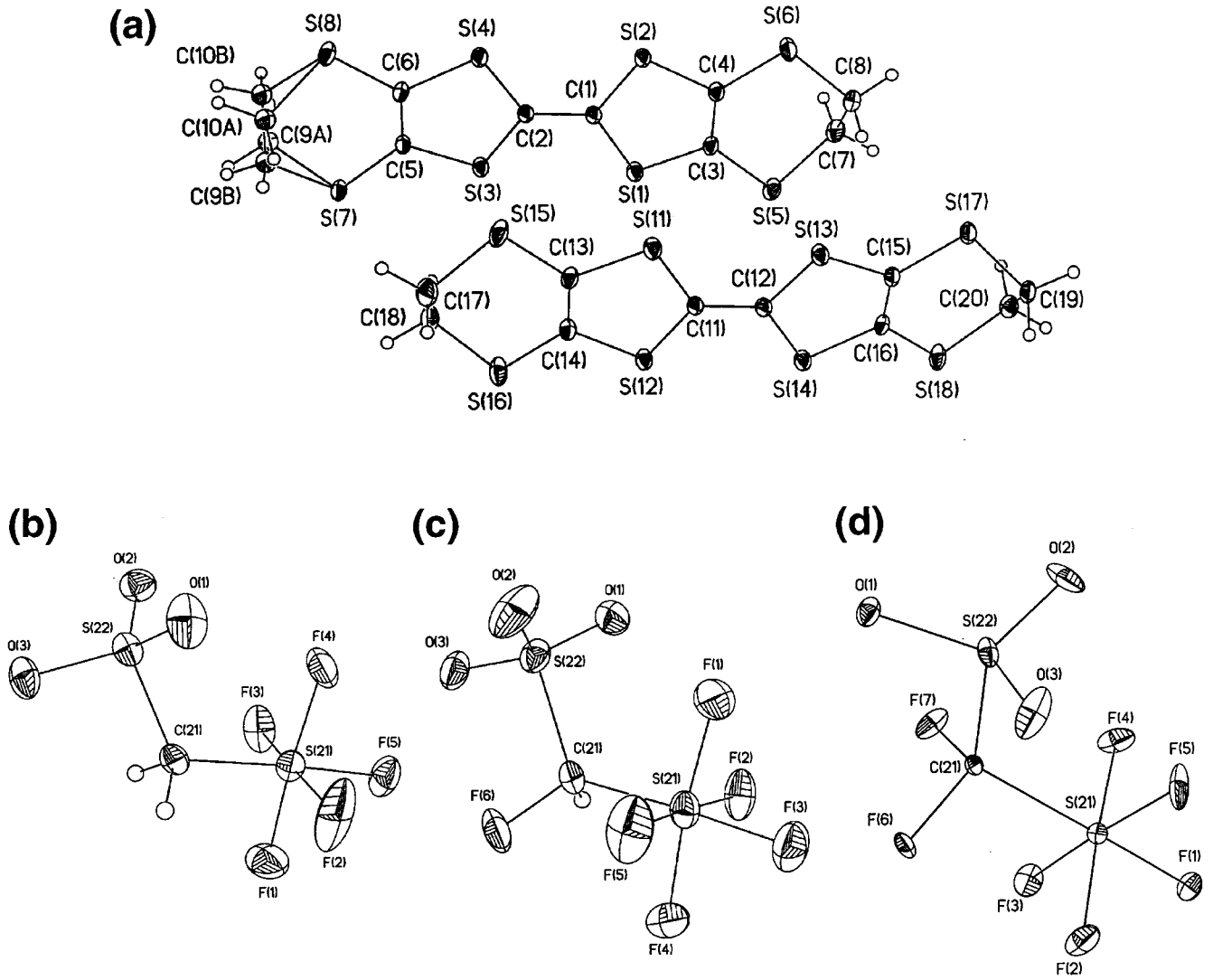

Figure 1. Atom labeling used for (a) the donor molecules in β''-$(ET)_2SF_5CH_2SO_3$, (b) the anion of β''-$(ET)_2SF_5CH_2SO_3$, (c) the anion of β''-$(ET)_2SF_5CHFSO_3$, and (d) the anion of β'-$(ET)_2SF_5CF_2SO_3$. Thermal displacement ellipsoids (50%) are shown except for the hydrogen atoms. The same atom labeling was applied to the donor molecules in the other two salts, except for the lack of ethylene group disorder.

ESR Spectroscopy. Single-crystal samples of β''-$(ET)_2SF_5CH_2SO_3$, β''-$(ET)_2SF_5CHFSO_3$, and β'-$(ET)_2SF_5CF_2SO_3$ were mounted on the cut edge of a quartz rod, and ESR measurements were performed using an IBM ER-200 X-band spectrometer equipped with a TE_{102} rectangular microwave cavity and an Oxford Instruments (Witney, England) ESR-900 flow-through cryostat with an ITC4 temperature controller. Temperature-dependent ESR data were obtained at 9.49 GHz with 100 kHz field modulation. Angular dependent spectra were recorded at room temperature with the use of a commercial goniometer.

Electrical Transport. Temperature-dependent electrical resistivity measurements of β''-$(ET)_2SF_5CH_2SO_3$, β''-$(ET)_2SF_5CHFSO_3$, and β'-$(ET)_2SF_5CF_2SO_3$ were made using a four-probe dc technique with a LakeShore Model 7000 cryostat equipped with RES7000 software. The current and voltage contacts in a linear arrangement were made with gold wire (0.0005 in. diameter) attached directly to the crystals with fast-drying silver paint (DuPont). Resistivity data were recorded during both the cooling and warming cycles, and a slow cooling/warming rate of about 1°/min was utilized to prevent microcracking of either the crystal sample or the contacts. Direct currents of 0.1, 0.25, and 0.001 mA were applied for β''-$(ET)_2SF_5CH_2SO_3$, β''-$(ET)_2SF_5CHFSO_3$, and β'-$(ET)_2SF_5CF_2SO_3$, respectively.

Magnetic Susceptibility. Single-crystal samples of β''-$(ET)_2SF_5CH_2SO_3$, β''-$(ET)_2SF_5CHFSO_3$, and β'-$(ET)_2SF_5CF_2SO_3$ were used to measure their ac susceptibilities on a LakeShore Model 7000 ac susceptometer equipped with a He subpot low-temperature option using a modulation frequency of 125 Hz and an ac field of 1 G. Samples were cooled from room temperature to 4 K over a period of 15 min, and then further cooled to 1.2 K. Our ac susceptibility measurements are consistent with the ESR results but do not possess a high enough sensitivity for detailed analysis. For each compound only a small amount of sample was available for ac susceptibility measurements.

III. Results and Discussion

Crystal Structures. As in most 2:1 salts of ET, layers of donor molecules are separated by layers of the anions in β''-$(ET)_2SF_5CH_2SO_3$, β''-$(ET)_2SF_5CHFSO_3$, and β'-$(ET)_2SF_5CF_2SO_3$. The donor molecule packing in β''-$(ET)_2SF_5CH_2SO_3$ and β''-$(ET)_2SF_5CHFSO_3$ has the tilted stacks of ET molecules of the β'' packing motif,[9,17,18,20,21] whereas β'-$(ET)_2SF_5CF_2SO_3$ has the dimerized stack pattern typical of the β' packing type.[14,15] There are two crystallographically nonequivalent ET molecules (hereafter designated as molecules A and B) in all three salts. Figure 1a shows the atom numbering used for the donor molecules of all three salts. Parts b, c, and d of Figure

Table 1. Crystallographic Data and Structure Refinement[a]

	crystal				
	β''-$(ET)_2SF_5CH_2SO_3$	β'-$(ET)_2SF_5CF_2SO_3$[b]	β'-$(ET)_2SF_5CF_2SO_3$	β''-$(ET)_2SF_5CHFSO_3$	β''-$(ET)_2SF_5CH_2CF_2SO_3$[c]
T, K	298	298	120	298	123
chemical formula	$(C_{10}H_8S_8)_2CH_2F_5O_3S_2$	$(C_{10}H_8S_8)_2CF_7O_3S_2$	$(C_{10}H_8S_8)_2CF_7O_3S_2$	$(C_{10}H_8S_8)_2CHF_6O_3S_2$	$(C_{10}H_8S_8)_2C_2H_2F_7O_3S_2$
formula wt, g	990.44	1026.42	1026.42	1008.43	1040.45
crystal system	triclinic	triclinic	triclinic	triclinic	triclinic
a, Å	8.8052(2)	7.862(2)	7.6994(2)	8.7965(2)	9.1536(6)
b, Å	11.7986(2)	13.222(3)	13.1514(2)	11.7264(2)	11.4395(8)
c, Å	17.7276(3)	17.660(5)	17.6425(4)	17.5763(4)	17.4905(12)
α, deg	75.884(1)	81.37(2)	81.323(1)	95.893(1)	94.316(1)
β, deg	86.163(1)	87.03(2)	87.416(1)	90.178(1)	91.129(1)
γ, deg	77.333(1)	75.33(2)	74.994(1)	102.286(1)	102.764(1)
V, Å^3	1742.45(1)	1755.6(9)	1705.74(1)	1761.55(1)	1779.9(2)
space group	$P\bar{1}$		$P\bar{1}$	$P\bar{1}$	$P\bar{1}$
Z	2		2	2	2
ρ_{calcd}, g cm^{-3}	1.888		1.998	1.901	1.941
S, goodness of fit	0.984		1.007	1.060	1.635
R_1 (%)/reflections	5.04		4.50	5.08	4.6
wR_2 (%)/reflections	14.74		11.61	13.78	4.5

[a] $R_1 = \sum(||F_o| - |F_c||)/\sum|F_o|$ for $F_o > 4\sigma(F_o)$; $wR_2 = [\sum[w(F_o^2 - F_c^2)^2]/\sum[w(F_o^2)^2]]^{1/2}$ for all reflections; $S = [\sum[w(F_o^2 - F_c^2)^2]/(n-p)]^{1/2}$; $w = 1/[\sigma^2(F_o^2)+(0.0370p)^2+0.31p]$, $p = [\max(F_o^2,0)+ 2F_c^2]/3$ [b] Unit cell determination only. [c] Taken from ref 9, refinement on F_o.

1 show the atom numbering used for the $SF_5CH_2SO_3^-$, $SF_5CHFSO_3^-$, and $SF_5CF_2SO_3^-$ anions, respectively. Table 1 summarizes the crystallographic data for β''-$(ET)_2SF_5CH_2SO_3$, β''-$(ET)_2SF_5CHFSO_3$, and β'-$(ET)_2SF_5CF_2SO_3$.

In β''-$(ET)_2SF_5CH_2SO_3$ at room temperature, the conformation of the terminal ethylene group (C9−C10) in molecule A is disordered with 70% occupation for the C9A and C10A positions (eclipsed), and 30% occupancy for the C9B and C10B positions (staggered). The donor layer of β''-$(ET)_2SF_5CH_2SO_3$ consists of ET molecule stacks running along the a direction, and molecules A and B alternate in each donor stack (Figure 2a). The donor stacks are arranged such that molecules A in different stacks form nearly coplanar arrays along the $(-a + b)$ direction, and so do molecules B. Intermolecular S···S contacts shorter than 3.6 Å (i.e., the sum of the sulfur van der Waals radii) are found between adjacent donor stacks, but not within donor stacks. The $SF_5CH_2SO_3^-$ anion of β''-$(ET)_2SF_5CH_2SO_3$ has a distorted tetrahedral geometry around the carbon atom with the S−C−S bond angle of 120.7(2)°. The F and O atoms of the anion make numerous contacts with the ethylene hydrogen atoms of ET molecules. Figure 3a shows a schematic view of the anion layer of β''-$(ET)_2SF_5CH_2SO_3$, which is made up of anion dimers. In each anion dimer, two anions are linked by two C−H···O hydrogen bonds (H···O = 2.284 Å) between one hydrogen atom of the CH_2 group and one O atom of the SO_3 group. The remaining oxygen atoms and the fluorine atoms of the terminal SF_5 groups make short C−H···O and C−H···F contacts with the ethylene hydrogen atoms of ET molecules. With the $SF_5CH_2SO_3^-$ anions, molecules A make predominantly short C−H···O contacts, while molecules B make mainly C−H···F contacts (see Table 2).

The donor layer of β''-$(ET)_2SF_5CHFSO_3$, shown in Figure 2b, has a packing motif similar to that found in β''-$(ET)_2SF_5CH_2SO_3$. However, each donor stack of β''-$(ET)_2SF_5CHFSO_3$, consists of only one kind of donor molecules, and stacks of molecules A alternate with stacks of molecules B along the interstack direction. Donor molecules A and B in adjacent stacks form nearly coplanar arrays along the $(a + b)$ direction. The intermolecular S···S contacts shorter than 3.6 Å occur between adjacent stacks, but not within stacks. The $SF_5CHFSO_3^-$ anion adopts a distorted tetrahedral geometry around the carbon atom with the S−C−S bond angle of 119.4(2)°. As in the anion layer of β''-$(ET)_2SF_5CH_2SO_3$, the anions of β''-$(ET)_2SF_5CHFSO_3$ form dimers (see Figure 3b) by making C−H···O hydrogen bonds between the hydrogen atom of the central carbon and one oxygen atom of the sulfonate group. As summarized in Table 2, molecules A and B make short C−H···O and C−H···F contacts with the anions. Unlike the case of β''-$(ET)_2SF_5CH_2SO_3$, however, molecules A and B in β''-$(ET)_2SF_5CHFSO_3$ make similar numbers of short C−H···O and C−H···F contacts.

In β'-$(ET)_2SF_5CF_2SO_3$ at 120 K there is no disorder in either the cation or anion layers. As shown in Figure 2c, the donor layer has stacks of molecules A that alternate with stacks of molecules B, and each donor stack consists of ET dimers. There are short intermolecular S···S contacts shorter than 3.6 Å between adjacent stacks, but not within donor stacks. The $SF_5CF_2SO_3^-$ anion of β'-$(ET)_2SF_5CF_2SO_3$ has a distorted tetrahedral geometry around the carbon atom with the S−C−S bond angle of 118.7(2)°. In β'-$(ET)_2SF_5CF_2SO_3$, the anions exist as monomers as depicted in Figure 3c. Donor molecules A make only short C−H···O contacts with the anion. Each molecule B has only one C−H···F contact shorter than 2.55 Å with the anions, and two C−H···O contacts shorter than 2.70 Å (Table 2).

It is noteworthy that for the β''-$(ET)_2SF_5CH_2SO_3$ and β''-$(ET)_2SF_5CHFSO_3$ salts C−H···O hydrogen bond interactions occur not only between the donor molecules and anions but also between the anions. For β'-$(ET)_2SF_5CF_2SO_3$ these interactions exist only between the donors and anions because no such interaction is possible between the anions. These observations confirm the importance of C−H···O hydrogen bond interactions in the packing of organic conducting salts.[29]

(29) Whangbo, M.-H.; Jung, D.; Ren, J.; Evain, M.; Novoa, J. J.; Mota, F.; Alvarez, S.; Williams, J. M.; Beno, M. A.; Kini, A. M.; Wang, H. H.; Ferraro, J. R. In *The Physics and Chemistry of Organic Superconductors*; Saito, G., Kagoshima, S., Eds.; Springer-Verlag: Berlin, Heidelberg, 1990; Vol. 51, p 262.

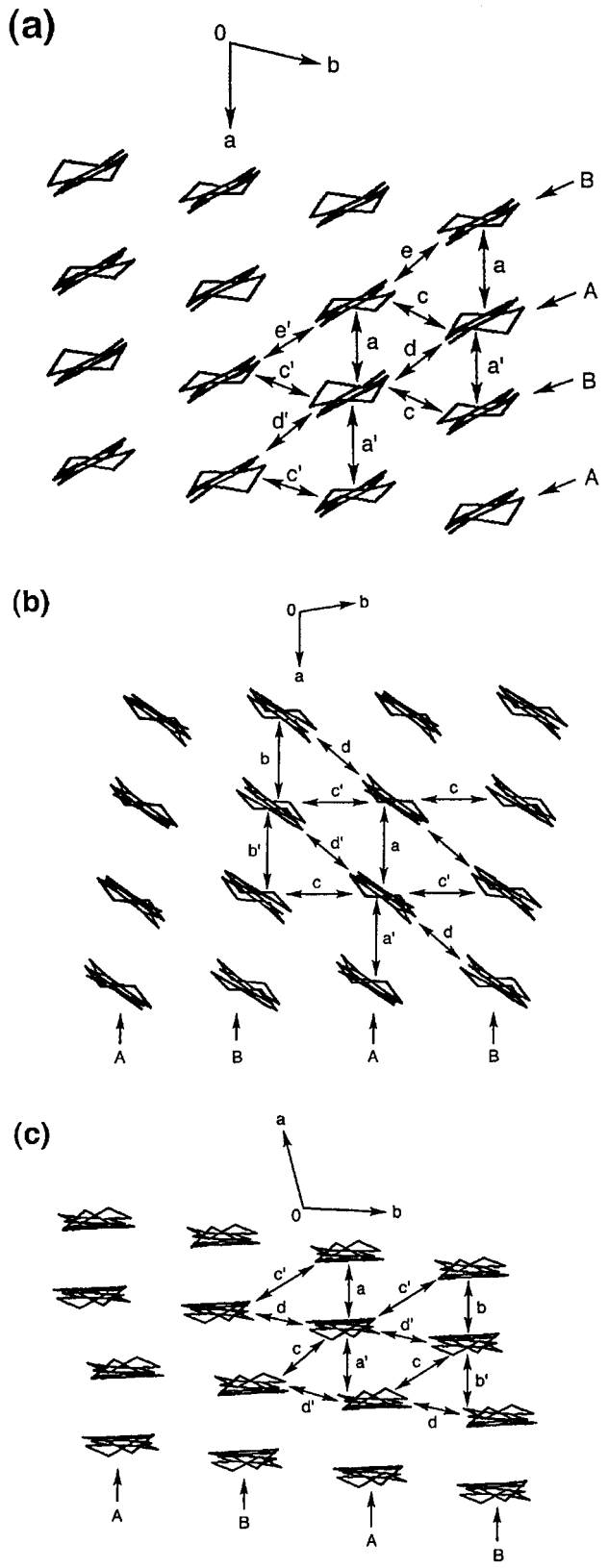

Figure 2. Packing patterns of the donor molecule layers of (a) β''-$(ET)_2SF_5CH_2SO_3$, (b) β''-$(ET)_2SF_5CHFSO_3$, and (c) β'-$(ET)_2SF_5CF_2SO_3$, where the labels (e.g., a, a', b, etc.) between adjacent ET molecules are used to specify the HOMO−HOMO interaction energies listed in Table 3.

The HOMO of the ET molecule is bonding in the C═C bonds but antibonding in the C−S bonds of the TTF moiety (Figure 4a). Thus, an increase in the charge q on the ET^{q+} cation increases the C═C bond lengths (a and d) but shortens the C−S bonds (b and c) of the TTF moiety (Figure 4b). By defining the bond length difference δ between the C−S and C═C bonds as

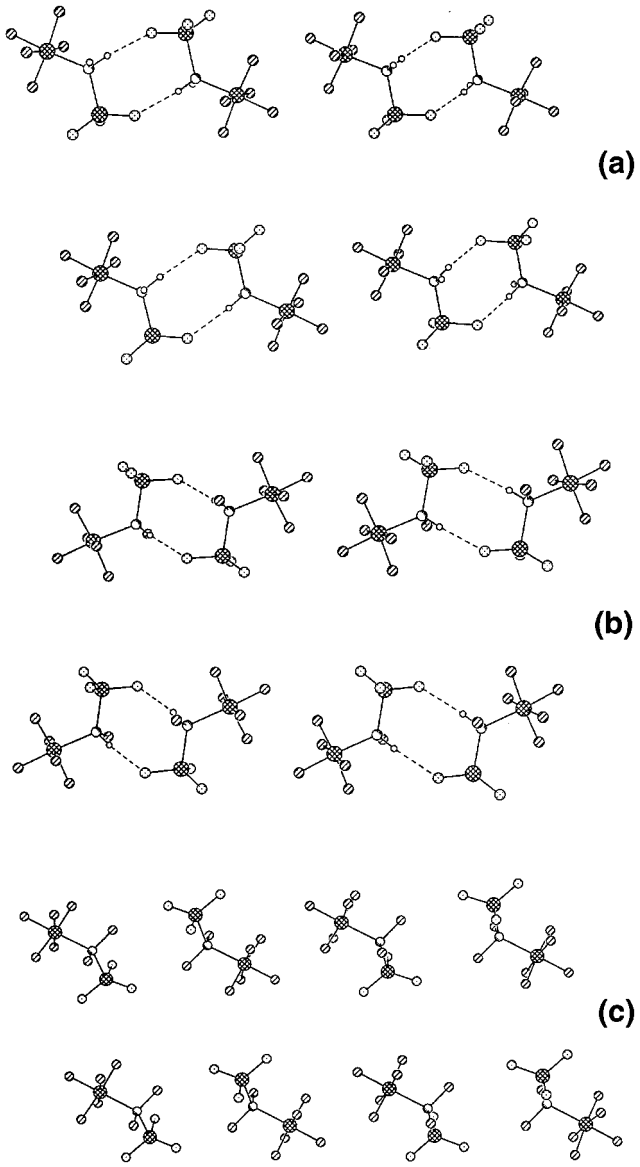

Figure 3. Packing patterns of the anion layers of (a) β''-$(ET)_2SF_5CH_2SO_3$, (b) β''-$(ET)_2SF_5CHFSO_3$, and (c) β'-$(ET)_2SF_5CF_2SO_3$.

$$\delta = (r_b + r_c) - (r_a + r_d) \qquad (1a)$$

where r_i refers to the length to the length of the bond i (= a, b, c, d), Guionneau et al.[30] recently found that the charge q is linearly related to δ as

$$q = 6.347 - 7.463\delta \qquad (1b)$$

On the basis of this relationship and the C═C and C−S bond lengths determined in the present study, the charges on molecules A and B of β''-$(ET)_2SF_5CH_2SO_3$ are calculated to be +0.94 and +0.72, respectively, indicating a significant difference in the oxidation state of each donor molecule. These numbers are scaled to +0.6 and +0.4, respectively, by requiring their sum

(30) Guionneau, P.; Kepert, C. J.; Bravic, G.; Chasseau, D.; Truter, M. R.; Kurmoo, M.; Day, P. *Synth. Met.* **1997**, *86*, 1973.

Table 2. Short Intermolecular C−H···O and C−H···F Contacts between the Ethylene Groups of ET Molecules and the $SF_5CH_2SO_3^-$, $SF_5CHFSO_3^-$ and $SF_5CF_2SO_3^-$ Anions in β''-$(Et)_2SF_5CH_2SO_3$, β''-$(Et)_2SF_5CHFSO_3$ and β'-$(Et)_2SF_5CF_2SO_3$[a]

	H···O (Å)		H···F (Å)	
salt	A	B	A	B
β''-$(ET)_2SF_5CH_2SO_3$	2.428[b]	2.591	2.592	2.343
	2.580[b]			2.430
	2.594[b]			2.452
	2.682[b]			
	2.422[c]			
	2.666[c]			
	2.674[c]			
β''-$(ET)_2SF_5CHFSO_3$	2.543	2.410	2.346	2.449
	2.612	2.668	2.528	2.449
β'-$(ET)_2SF_5CF_2SO_3$	2.496	2.590		2.406
	2.506	2.640		
	2.507			
	2.592			

[a] Only the H···O and H···F distances shorter than 2.70 and 2.55 Å, respectively, are listed. [b] Calculated using the (C9A, C10A) conformation of the ET molecule A. [c] Calculated using the (C9B, C10B) conformation of the ET molecule A.

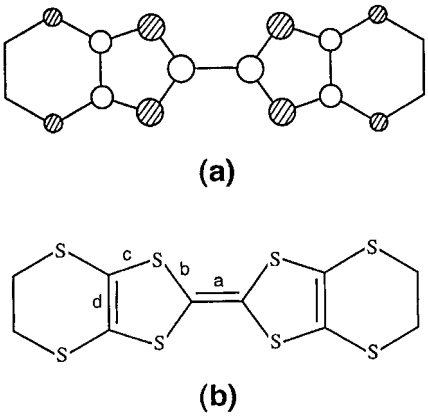

Figure 4. (a) Nodal properties of the HOMO of ET and (b) C═C and C−S bond labels of ET used for the q vs δ relationship.

to be normalized to +1.0. It is important to note that the charged ends of the $SF_5CH_2SO_3^-$ (i.e., the SO_3^- groups) anions arrange themselves toward the more charged $ET^{+0.6}$ cations, and the SF_5 moiety toward the less charged $ET^{+0.4}$ cations. Charge localization due to electrostatic interactions was also found in other organic conducting salts.[31,32] The charges on molecules A and B of β''-$(ET)_2SF_5CHFSO_3$ are calculated to be +0.64 and +0.71, respectively, which are scaled to +0.47 and +0.53, respectively. The charges on molecules A and B of β'-$(ET)_2SF_5CF_2SO_3$ are calculated to be equal at +0.59, which is scaled to +0.5 each. Thus, the charge states on molecules A and B are similar in β''-$(ET)_2SF_5CHFSO_3$ and β'-$(ET)_2SF_5CF_2SO_3$, but considerably different in β''-$(ET)_2SF_5CH_2SO_3$.

Physical Properties. The temperature-dependent electrical resistivities measured for β'-$(ET)_2SF_5CF_2SO_3$, β''-$(ET)_2SF_5CH_2SO_3$, and β''-$(ET)_2SF_5CHFSO_3$ are presented in Figures 5 and 6. β'-$(ET)_2SF_5CF_2SO_3$ is semiconductive between 100 and 298 K with $E_a = 110$ meV and a room-temperature conductivity of 7.9×10^{-4} S/cm (Figure 5a). β''-$(ET)_2SF_5CH_2SO_3$ is also a semiconductor between 100 and 298 K with $E_a = 56$ meV and a room-temperature conductivity of 5.3×10^{-2} S/cm (Figure 5b). β''-$(ET)_2SF_5CHFSO_3$ is semiconducting between room temperature and 100 K, is metallic between 100 and 6 K, and undergoes a metal-to-semiconductor transition below 10 K (Figure 6).

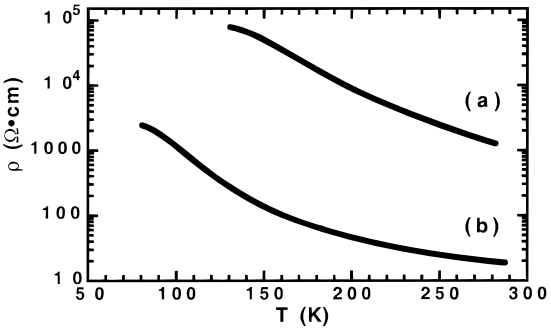

Figure 5. Temperature dependence of the electrical resistivity measured for single crystals of (a) β'-$(ET)_2SF_5CF_2SO_3$ and (b) β''-$(ET)_2SF_5CH_2SO_3$.

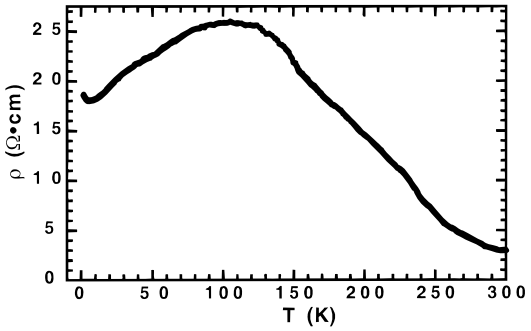

Figure 6. Temperature dependence of the electrical resistivity measured for a single crystal of β''-$(ET)_2SF_5CHFSO_3$.

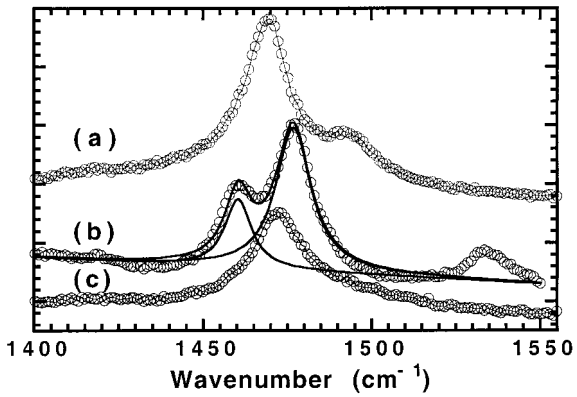

Figure 7. Raman spectra measured for single crystals of (a) β'-$(ET)_2SF_5CF_2SO_3$, (b) β''-$(ET)_2SF_5CH_2SO_3$, and (c) β''-$(ET)_2SF_5CHFSO_3$. (Spectra are offset for clarity.)

The Raman spectra of β'-$(ET)_2SF_5CF_2SO_3$, β''-$(ET)_2SF_5CH_2SO_3$, and β''-$(ET)_2SF_5CHFSO_3$ are shown in Figure 7, which highlights only the ν_3 (A_g) mode that involves the stretching vibration of the central C═C double bond of ET.[33,34] The charge q on the ET^{q+} cation

(31) Ren, J.; Evain, M.; Whangbo, M.-H.; Beno, M. A.; Geiser, U.; Kini, A. M.; Wang, H. H.; Williams, J. M. *Solid State Commun.* **1989**, *70*, 615.
(32) Kepert, C. J.; Kurmoo, M.; Day, P. *J. Mater. Chem.* **1997**, *7*, 221.
(33) Wang, H. H.; Ferraro, J. R.; Williams, J. M.; Geiser, U.; Schlueter, J. A. *J. Chem. Soc., Chem. Commun.* **1994**, 1893.
(34) Eldridge, J. E.; Homes, C. C.; Williams, J. M.; Kini, A. M.; Wang, H. H. *Spectrochim. Acta* **1995**, *51A*, 947.

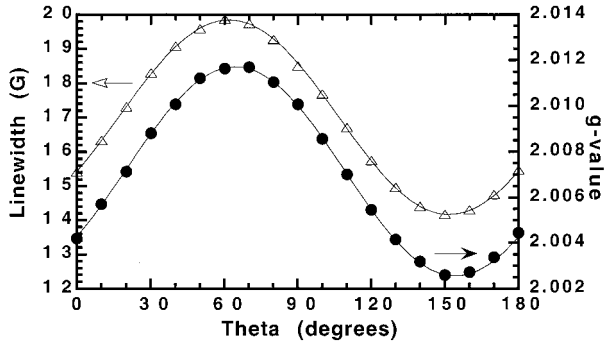

Figure 8. Angular dependence of the line width ΔH and the g value determined for β''-$(ET)_2SF_5CH_2SO_3$ at 298 K.

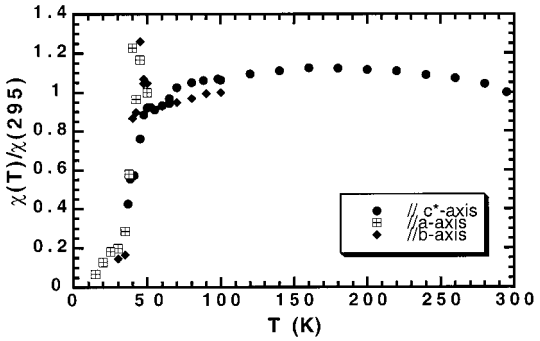

Figure 9. Temperature dependence of the relative spin susceptibility, of β'-$(ET)_2SF_5CF_2SO_3$ with the magnetic field oriented along three approximately othogonal directions.

in an ET salt can be inferred from the ν_3 frequency independently of estimates from the bond lengths (see above).[33] Electron removal from the HOMO of an ET molecule weakens the C=C bond, hence it reduces the C=C stretching vibration frequency ν_3. β'-$(ET)_2SF_5CF_2SO_3$ and β''-$(ET)_2SF_5CHFSO_3$ each have a peak corresponding to the ν_3 mode at 1469 cm^{-1} (Figure 7a) and 1471 cm^{-1} (Figure 7c), respectively. In β''-$(ET)_2SF_5CH_2SO_3$, the peak corresponding to the ν_3 mode is split into two subpeaks at 1476.8 and 1460.4 cm^{-1} (Figure 7b). A linear correlation between q and ν_3 in ET salts has been found earlier,[33] hence the subpeaks at 1476.8 and 1460.4 cm^{-1} correspond to fractional charges of 0.38 and 0.54, respectively. These values may be scaled to be +0.41 and +0.59 by requiring their sum to be normalized to +1.0. These values are in excellent agreement with the corresponding results determined from the crystal structure analysis (see above).

β'-$(ET)_2SF_5CF_2SO_3$, β''-$(ET)_2SF_5CH_2SO_3$, and β''-$(ET)_2SF_5CHFSO_3$ were characterized by ESR spectroscopy. The line width ΔH and the g value associated with an ESR peak depend on the orientation of the ET molecules with respect to the magnetic field. As a representative example, Figure 8 shows an orientation dependence of the ΔH and g value recorded for β'-$(ET)_2SF_5CH_2SO_3$. Here the plane of the donor layer is parallel to the magnetic field when the angle $\theta = 0°$, and perpendicular to the magnetic field when $\theta = 90°$. The orientation dependence of the ΔH and g value shows that the line width ranges for β'-$(ET)_2SF_5CF_2SO_3$, β''-$(ET)_2SF_5CH_2SO_3$, and β''-$(ET)_2SF_5CHFSO_3$ are 7−11, 14−20, and 26−38 G, respectively. The narrower line width for β'-$(ET)_2SF_5CF_2SO_3$ is typical of β'-type salts (e.g., β'-$(ET)_2ICl_2$ and β'-$(ET)_2AuCl_2$), and the line width of β''-$(ET)_2SF_5CHFSO_3$ is consistent with those of other β''-type salts, e.g. β''-$(ET)_2SF_5CH_2CF_2SO_3$ (23−34 G) and β''-$(ET)_4(H_3O)Fe(C_2O_4)_3(C_6H_5CN)$ (23−35 G). However, the line width of β''-$(ET)_2SF_5CH_2SO_3$ deviates considerably from those of other β''-type salts. The g value ranges for β'-$(ET)_2SF_5CF_2SO_3$, β''-$(ET)_2SF_5CH_2SO_3$, and β''-$(ET)_2SF_5CHFSO_3$ are 2.000−2.008, 2.002−2.012, and 2.004−2.014, respectively. For all three compounds the orientation dependence of the g value is in-phase with that of the line width ΔH, as in Figure 8. This behavior is typical of β-like samples. The maximum g value in these compounds (2.012) occurs when the magnetic field is along the direction of the central C=C bond of the ET molecule, and the minimum g value (2.000) occurs when the magnetic field is along the direction perpendicular to the molecular plane of the ET molecule.

Low-temperature ESR studies were also carried out for β''-$(ET)_2SF_5CH_2SO_3$, β'-$(ET)_2SF_5CF_2SO_3$, and β''-$(ET)_2SF_5CHFSO_3$. With decreasing temperature, both the line width and the spin susceptibility of β''-$(ET)_2SF_5CH_2SO_3$ decrease monotonically (not shown). The line width decreases from 19 G at room temperature to 2 G at 30 K at which temperature the relative spin susceptibility is 5% of its room-temperature value. The decrease of the spin susceptibility with decreasing temperature suggests a thermal activation process associated with an energy gap. A plot of the log value of the spin susceptibility versus the inverse temperature ($1/T$) between 295 and 150 K leads to an activation energy of 8.2 meV for β''-$(ET)_2SF_5CH_2SO_3$. Thus, the ESR susceptibility data are consistent with the four-probe electrical resistivity measurements in that β''-$(ET)_2SF_5CH_2SO_3$ is a semiconductor although the activation energies derived from the two methods are not identical. Figure 9 shows the spin susceptibility of β'-$(ET)_2SF_5CF_2SO_3$ as a function of temperature. The circles represent the data obtained when the magnetic field was perpendicular to the plane of the donor layer (i.e., parallel to the c^* axis). The squares and diamonds refer to the data obtained with the magnetic field aligned along the a and b axis, respectively. Upon lowering the temperature, the relative spin susceptibility (filled circles) increases slightly from room temperature to a maximum at 160 K, and then decreases slowly to its room temperature value at 60 K. Between 60 and 45 K, the spin susceptibility continues to decrease, and below 45 K a rapid decrease is observed. As the temperature is lowered, the line width (not shown) decreases monotonically from 11 G at room temperature to 0.9 G at 60 K. The line width is nearly the same between 60 and 45 K, and rapidly increases below 45 K. The measurements along the a and b axis indicate a rapid increase in $\chi(T)$ with decreasing temperature between 50 and 45 K, followed by a precipitous drop in $\chi(T)$ below 45 K. The spin susceptibility decreases to ~15% of its room-temperature value at 30 K. The rapid decrease in the spin susceptibility of β'-$(ET)_2SF_5CF_2SO_3$ in all three directions below 45 K indicates the occurrence of a spin gap, and is not consistent with a three-dimensional (3D) antiferromagnetic (AFM) ordering as found for β'-$(ET)_2ICl_2$ (T_N = 22 K) and β'-$(ET)_2AuCl_2$ (T_N = 28 K).[35] In β'-$(ET)_2SF_5CF_2SO_3$ each dimer unit $(ET)_2^+$ carries an unpaired spin, and the

(35) Yoneyama, N.; Miyazaki, A.; Enoki, T.; Saito, G. *Synth. Met.* **1997**, *86*, 2029.

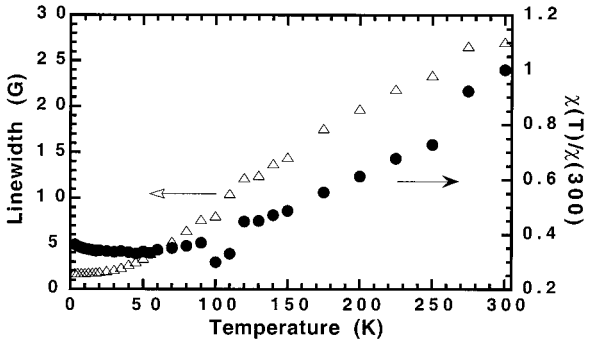

Figure 10. Temperature dependence of the ESR line width and relative spin susceptibility of β''-$(ET)_2SF_5CHFSO_3$ determined with the magnetic field perpendicular to the plane of the donor layers (*ab* plane).

interactions between these dimers in each donor layer are anisotropic (see below). Therefore, it is possible that the cause for a spin gap in β'-$(ET)_2SF_5CF_2SO_3$ below 45 K is a spin−Peierls transition.[36−41]

Figure 10 shows the ESR line width and relative spin susceptibility of β''-$(ET)_2SF_5CHFSO_3$ as a function of temperature. With decreasing temperature from 298 to 100 K, the spin susceptibility of β''-$(ET)_2SF_5CHFSO_3$ diminishes gradually, thereby indicating a semiconducting behavior. From 100 K to about 20 K, the spin susceptibility remains nearly constant, which indicates a metallic behavior. When the temperature is lowered below about 12 K, the spin susceptibility slightly increases again. The latter indicates that electron localization takes place leading to a paramagnetic ground state. A possible cause for this localization is that the reduction of the unit cell volume at low temperatures makes the extent of dimerization stronger in each donor stack so that each donor dimer becomes a spin center. To test this speculation, it is necessary to determine the single-crystal structure of β''-$(ET)_2SF_5CHFSO_3$ at a very low temperature. The ESR susceptibilities of β''-$(ET)_2SF_5CHFSO_3$ are consistent with the transport properties found in the electrical resistivity measurements.

Electronic Structures. The strength of the interaction between nearest-neighbor ET molecules in a given donor layer can be estimated by calculating the HOMO−HOMO interaction energy β_{ij} [42]

$$\beta_{ij} = \langle \psi_i | H^{\text{eff}} | \psi_j \rangle \qquad (2)$$

where H^{eff} is an effective Hamiltonian, and ψ_i and ψ_j are the HOMO's of ET molecules *i* and *j*, respectively. Figure 2a−c and Table 3 summarize the β_{ij} values calculated for all nearest-neighbor donor pairs in the donor layers of β''-$(ET)_2SF_5CH_2SO_3$, β''-$(ET)_2SF_5CHFSO_3$, and β'-$(ET)_2SF_5CF_2SO_3$ by use of the extended Hückel tight binding method.[43,44] For the purpose of comparison, Table 3 also lists the β_{ij} values calculated for the donor layers of β'-$(ET)_2AuCl_2$ and β'-$(ET)_2ICl_2$.

Table 3. HOMO−HOMO Interaction Energies) between the Nearest-Neighbor ET Molecules in the Donor Molecule Layers of β''-$(Et)_2SF_5CH_2SO_3$, β''-$(Et)_2SF_5CHFSO_3$ and β'-$(Et)_2SF_5CF_2SO_3$

	β_{ij}, meV	
salt	intrastack	interstack
β''-$(ET)_2SF_5CH_2SO_3$	$a = 85$	$c = 260$
	$a' = 12$	$c' = 265$
		$d = 118$
		$d' = 130$
		$e = 144$
		$e' = 126$
β''-$(ET)_2SF_5CHFSO_3$	$a = 35$	$c = 283$
	$a' = 95$	$c' = 255$
	$b = 86$	$d = 124$
	$b' = 100$	$d' = 138$
β'-$(ET)_2SF_5CF_2SO_3$	$a = 601$	$c = 200$
	$a' = 96$	$c' = 73$
	$b = 569$	$d = 115$
	$b' = 63$	$d' = 110$
β'-$(ET)_2AuCl_2$ [a]	$a = 477$	$c = 195$
	$a' = 53$	$c' = 89$
	$b = 477$	$d = 74$
	$b' = 53$	$d' = 74$
β'-$(ET)_2ICl_2$[a]	$a = 508$	$c = 189$
	$a' = 40$	$c' = 86$
	$b = 508$	$d = 64$
	$b' = 40$	$d' = 64$

[a] In terms of the repeat vectors of these salts, the intrastack and interstack directions are given by the $(a + b)$ and *a* directions, respectively. The interaction energies of these salts were listed on the basis of the packing diagram of Figure 2c for the purpose of comparison with the β''-$(ET)_2SF_5CF_2SO_3$ salt.

In β''-$(ET)_2SF_5CH_2SO_3$, the intrastack interactions are significantly weaker than the interstack interactions. The strongest interaction between stacks occurs along the *b* axis direction between molecules A and B as evidenced by the structure and spectroscopic data (see above). Molecules A and B are substantially different in their charges, and hence the HOMO energies of molecules A and B differ considerably (by 0.17 eV). This situation is conducive for electron localization and is probably responsible for the semiconducting property of β''-$(ET)_2SF_5CH_2SO_3$. Other β''-$(ET)_2X$ salts (X = $AuBr_2^-$, $IAuBr^-$, $SF_5CH_2CF_2SO_3^-$, $[Fe(C_2O_4)_3]^{3-}$, and $[Cr(C_2O_4)_3]^{3-}$)[9,17−19,21,22] have more evenly charged ET molecules and are metallic (in some cases superconducting) to low temperatures.

Similarly in β''-$(ET)_2SF_5CHFSO_3$, the intrastack interactions are significantly weaker than the interstack interactions, and the strongest interaction between stacks occur along the *b* axis direction between molecules A and B. However, the two molecules have very similar charges, so that the HOMO energies of molecules A and B are essentially the same. This situation allows for electron delocalization, and metallic proper-

(36) Bray, J. W.; Hart, H. R.; Interrante, L. V., Jr.; Jacobs, I. S.; Kasper, J. S.; Watkins, G. D.; Wees, S. H.; Bonner, J. C. *Phys. Rev. LEtt.* **1975**, *35*, 744.
(37) Jacobs, I. S.; Bray, J. W.; Hart, H. R.; Interrante, L. V., Jr.; Kasper, J. S.; Watkins, G. D.; Prober, D. E.; Bonner, J. C. *Phys. Rev. B: Condens. Matter* **1976**, *14*, 3036.
(38) Huizinga, S.; Kommandeur, J.; Sawatzky, G. A.; Thole, B. T.; Kopinga, K.; de Jonge, W. J. M.; Roos, J. *Phys. Rev. B: Condens. Matter* **1979**, *19*, 4723.
(39) Obertelli, S. D.; Friend, R. H.; Talham, D. R.; Kurmoo, M.; Day, P. *J. Phys.: Condens. Matter* **1989**, *1*, 5671.
(40) Hase, M.; Teresaki, I.; Uchinokura, K. *Phys. Rev. Lett.* **1993**, *70*, 3651.
(41) Ueda, Y. *Chem. Mater.* **1998**, *10*, 2653.
(42) Whangbo, M.-H.; Williams, J. M.; Leung, P. C. W.; Beno, M. A.; Emge, T. J.; Wang, H. H. *Inorg. Chem.* **1985**, *24*, 3500.
(43) Whangbo, M.-H.; Hoffmann, R. *J. Am. Chem. Soc.* **1978**, *100*, 6093.
(44) Ren, J.; Liang, W.; Whangbo, M.-H. *Crystal and Electronic Structure Analysis Using CAESAR*; PrimeColor Software, Inc.: Cary, NC, 1998. (This book can be downloaded free of charge from the website, http://www.PrimeC.com/).

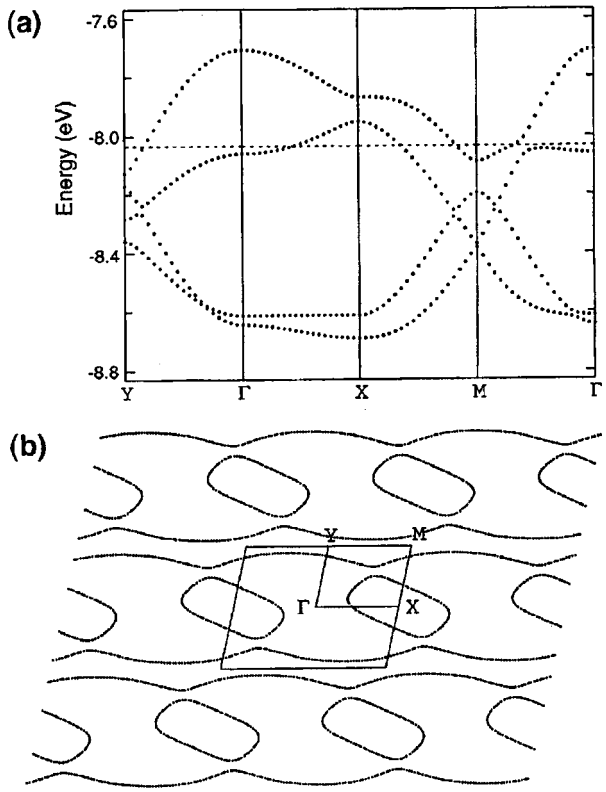

Figure 11. Electronic band structure of β''-$(ET)_2SF_5CHFSO_3$: (a) dispersion relations of the four highest occupied bands, and (b) Fermi surfaces associated with the two partially filled bands of part a. $\Gamma = (0, 0)$; $X = (a^*/2, 0)$; $Y = (0, b^*/2)$; and $M = (a^*/2, b^*/2)$.

ties are observed in β''-$(ET)_2SF_5CHFSO_3$. Figure 11a shows the dispersion relations of the four highest occupied bands calculated for β''-$(ET)_2SF_5CHFSO_3$. The highest-lying two bands are partially filled, and the Fermi surfaces associated with these two bands are shown in Figure 11b in an extended zone scheme. Within the first primitive zone, the Fermi surfaces consist of a hole pocket centered at X and a pair of wavy lines straddling the M → Y line. Thus, β''-$(ET)_2SF_5CHFSO_3$ has both one-dimensional (1D) and 2D Fermi surfaces. These features are similar to those found for β''-$(ET)_2SF_5CH_2CF_2SO_3$.[45,46]

Figure 2c and Table 3 reveal that the donor molecules of β'-$(ET)_2SF_5CF_2SO_3$ are strongly dimerized, and so are the donor molecules of β'-$(ET)_2AuCl_2$ and β'-$(ET)_2ICl_2$. The three salts have a similar pattern of HOMO−HOMO interactions, and these interactions are anisotropic within the plane of the donor layer. The primary difference between the three salts lie in the β_d and $\beta_{d'}$ values along the interstack direction, which increase in the order, β'-$(ET)_2ICl_2$ < β'-$(ET)_2AuCl_2$ < β'-$(ET)_2SF_5CF_2SO_3$.

IV. Conclusions

Although the $SF_5CX_2SO_3^-$ (X = H, F) anions differ in structure only slightly at the CX_2 group, their ET salts β''-$(ET)_2SF_5CH_2SO_3$, β''-$(ET)_2SF_5CHFSO_3$, and β'-$(ET)_2SF_5CF_2SO_3$ are considerably different in their crystal structures, physical properties, and electronic structures. β''-$(ET)_2SF_5CH_2SO_3$ and β''-$(ET)_2SF_5CHFSO_3$ have anion layers made up of anion dimers linked by two C—H···O hydrogen bonds, whereas the anion layer of β'-$(ET)_2SF_5CF_2SO_3$ consists of monomeric forms of anions. In contrast to the case of β''-$(ET)_2SF_5CHFSO_3$ and β'-$(ET)_2SF_5CF_2SO_3$, the two kinds of donor molecules in β''-$(ET)_2SF_5CH_2SO_3$ have considerably different charge densities thus favoring electron localization and leading to semiconducting properties. The donor molecules are strongly dimerized in β'-$(ET)_2SF_5CF_2SO_3$, and the interactions between the dimers are not strong, so that the ET dimers of β'-$(ET)_2SF_5CF_2SO_3$ act as spin centers. The ESR data of β'-$(ET)_2SF_5CF_2SO_3$ determined with the magnetic field aligned *a*, *b*, and *c** directions all show a sharp drop below 45 K, thus indicating the occurrence of a spin gap. The transport properties of β''-$(ET)_2SF_5CHFSO_3$ are somewhat complex. It shows a resistivity maximum around 100 K, is metallic below 100 K, and becomes nonmetallic below 6 K. The occurrence of the resistivity maximum around 100 K, also observed in a number of other ET salts including some superconductors,[47] is not well understood, although it appears to depend on the rate of cooling or warming a sample in electrical resistivity measurements as well as sample quality.[47,48] The MI transition below 6K is caused by electron localization leading to a paramagnetic ground state.

Acknowledgment. Work at Argonne National Laboratory was supported by the US Department of Energy, Office of Basic Energy Sciences, Division of Materials Sciences, under contract No. W-31-109-ENG-38. Work at Portland State University is supported by NSF grant No. CHE-9632815 and the Petroleum Research Fund ACS-PRF 31099-AC1. Work at North Carolina State University was supported by the U.S. Department of Energy, Office of Basic Sciences, Division of Materials Sciences, under Grant DE-FG05-86ER45259.

Supporting Information Available: Experimental details and tables of bond distances and angles, anisotropic displacement parameters, hydrogen coordinates and isotropic displacement parameters, and structural factors for compounds β''-$(ET)_2SF_5CH_2SO_3$, β''-$(ET)_2SF_5CHFSO_3$, and β'-$(ET)_2SF_5CF_2SO_3$ (CIF). This material is available free of charge via the Internet at http://pubs.acs.org.

CM990238Q

(45) Beckmann, D.; Wanka, S.; Wosnitza, J.; Schlueter, J.; Williams, J. M.; Nixon, P. G.; Winter, R. W.; Gard, G. L.; Ren, J.; Whangbo, M.-H. *Eur. Phys. J. B* **1998**, *1*, 295.

(46) Wang, H. H.; VanZile, M. L.; Schlueter, J. A.; Geiser, U.; Kini, A. M.; Sche, P. P.; Koo, H. T.; Whangbo, M.-H.; Nixon, P. G.; Winter, R. W.; Gard, G. L. *J. Phys. Chem.* **1999**, *103*, 5493.

(47) Su, X.; Zuo, F.; Schlueter, J. A.; Kelly, M. E.; Williams, J. M. *Phys. Rev. B: Condens. Matter* **1998**, *57*, R14056.

(48) Su, X.; Zuo, F.; Schlueter, J. A.; Kini, A. M.; Williams, J. M. *Phys. Rev. B: Condens. Matter* **1998**, *58*, R2944.